Multiscale and Multiphysics 1D Modeling of Polymer Electrolyte Membrane Water Electrolysers

Simone PIEROBON[a], Roberta TITTARELLI[b], Zhongliang LI[a]
[a]Université Marie et Louis Pasteur, CNRS, institut FEMTO-ST, F-90000 Belfort, France
[b]Université Marie et Louis Pasteur, SUPMICROTECH, CNRS, institut FEMTO-ST, F-25000 Besançon, France

ABSTRACT – This paper presents a one-dimensional multiphysics model for polymer electrolyte membrane water electrolysers. Our approach integrates mass transport equations in porous media and charge balance dynamics across the membrane electrode assembly. The model is partially implemented using the computing platform *FEniCS* and is compared with experimental I-V curves and a 0D model.

Mots-clés – multiphysics modeling, PEM water electrolysis, transport phenomena

1. INTRODUCTION

In this work, a 1D multiphysics model for *polymer electrolyte membrane water electrolysers* (PEMWE) is presented, allowing to study how to improve the durability of PEMWE. The durability of PEMWE relies on the intrinsic condition of its key components, indeed, the performance degradation of the *membrane electrode assembly* (MEA) is relevant component to study [1]: it includes thermal, mechanical, and chemical degradation of the membrane, the ionomer in the catalyst layers, the catalyst, the catalyst support and the liquid gas diffusion layers [2]. As a matter of fact, the degradation mechanisms in the MEA are strongly coupled to its local thermodynamic conditions [3], so an informative model is needed, to take them into account, when a degradation diagnosis and control strategy is developed. This becomes even more significant when considering that it has been chosen to use electricity generated from renewable sources, which are inherently intermittent: this amplifies the urgency for effective PEMWE control strategies [4].

The aim of the multiphysics model proposed is to help for the understanding and the caracterization of the degradation process in a PEMWE. More generally, our strategy focuses on developing methods to optimize operating conditions, minimizing material degradation and extending the PEMWE system's lifespan. In particular, the presented work is part of the project DuraPEME[1], which aims to improve the durability of PEMWE by developing an artificial intelligence accelerated multiscale degradation model.

We have hypothesized that the degradation process in PEMWE is closely related to phase transitions within the system, and we intend to validate this hypothesis through our research. Manufacturers typically guarantee a lifespan based on fixed operating conditions, but frequent variations in these conditions can significantly affect degradation.

Section 2 presents the governing equations for mass transport and charge balance, together with the key modeling assumptions. Section 3 describes the numerical implementation in FEniCS and the algorithm used to solve the multiphysics system. Section 4 shows the results of the numerical simulations and compares them with experimental data and a 0D model. Finally, Section 5 provides conclusions and outlines future research directions.

[1] https://anr.fr/Project-ANR-23-CE05-0002

2. MODEL

We are interested in the description of multiphase flow and transport phenomena [5] in the porous media [6] given by a module of PEMWE, represented in Figure 1.

The physical phenomena take place between the *porous transport layers* (domains Ω_{cPTL} and Ω_{aPTL}), the *catalyst layers* (domains Ω_{aCL} and Ω_{cCL}) and the *membrane* (PEM) of the PEMWE (domain Ω_M). This section focus on the partial differential equations (PDEs) describing these phenomena and the chosen assumptions to obtain a one-dimensional model. Proper boundary and initial conditions are given, even not specified here, in order to obtain a well posed problem.

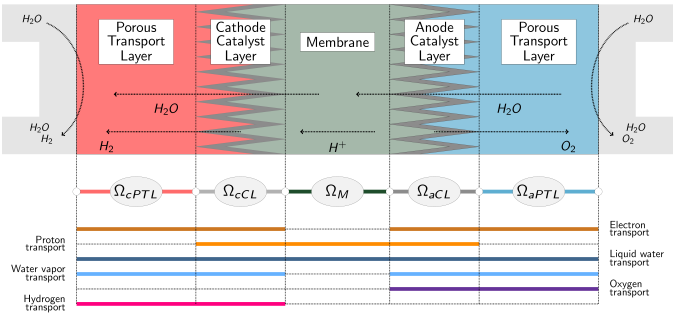

Figure 1. Top: Visual representation of the PEMWE and its components.
Middle: Illustration of the one-dimensional domain.
Bottom: Distribution of the different phenomena in the various subdomains.

2.1. *Physical equations*

The mass transport phenomena are different inside and outside the membrane, so the governing equations are different in the different subdomains. Firstly, we consider the cathode $\Omega_{cPTL} \cup \Omega_{cCL}$ and anode $\Omega_{aCL} \cup \Omega_{aPTL}$ subdomains. For a specie ι (H_2, O_2 or H_2O) in a phase α (gas or liquid), the general *compositional formulation* of the *mass balance equation* is

$$\frac{\partial}{\partial t}\left(\varepsilon s_\alpha \rho_\alpha \omega_\alpha^\iota\right) = -\nabla \cdot \left(\mathbf{j}_\alpha^\iota + \rho_\alpha \omega_\alpha^\iota \mathbf{u}_\alpha\right) + \mathcal{J}_\alpha^\iota + \mathcal{R}_\alpha^\iota \,, \quad (1)$$

where ε is the porosity of the porus medium, s_α is phase saturation, ρ_α is the phase density, ω_α^ι is the mass fraction of the specie in the phase, $\mathbf{u}_\alpha$ is the phase physical velocity, $\mathbf{j}_\alpha^\iota$ is the nonadvective flux vector, accounting for dispersive and diffusive transport, $\mathcal{J}_\alpha^\iota$ is the interphase mass transport term, $\mathcal{R}_\alpha^\iota$ is the specie chemical reaction term.

Dealing with porous media, the velocity field is given by the *Darcy's law* for momentum conservation in each phase [6]:

$$\mathbf{u}_\alpha = -K \frac{k_\alpha}{\mu_\alpha} \nabla p_\alpha \,, \quad (2)$$

where K is the absolute permeability of porous medium, k_α is the relative permeability of the phase, which depends only

on saturation, μ_α is the phase viscosity and p_α is the (partial) pressure of the phase. For the same reason, the nonadvective flux $\mathbf{j}_\alpha^\iota$ is expressed in Fickian form [6]:

$$\mathbf{j}_\alpha^\iota = -\varepsilon \rho_\alpha s_\alpha \mathbf{D}_\alpha^\iota \nabla \omega_\alpha^\iota \,, \tag{3}$$

where $\mathbf{D}_\alpha^\iota$ is a "macroscopic second-order tensor which is a function of molecular diffusion coefficient and fluid velocity".

In order to recover the phase balance laws, following the theoretical procedure detailed in [5], a summation of (1) over all species in the same phase yields

$$\frac{\partial}{\partial t}\left(\varepsilon s_\alpha \rho_\alpha\right) = -\nabla \cdot \left(\rho_\alpha \mathbf{u}_\alpha\right) + \mathcal{J}_\alpha \,, \tag{4}$$

where $\mathcal{J}_\alpha = \sum_\iota \mathcal{J}_\alpha^\iota$.

Inside the membrane (domain Ω_M), the mass transport is coupled with the ions transport. The governing equations are following, recovered from [7]:

$$\nabla \cdot N = 0 \quad N = \frac{\kappa_I \psi}{F} \nabla \phi_e - \left(\xi + \frac{\kappa_I \psi^2}{F^2}\right) \overline{V}_{H_2O} \nabla p_l \,, \tag{5}$$

$$\nabla \cdot i_e = 0 \quad i_e = -\kappa_I \nabla \phi_e - \frac{\kappa_I \psi}{F} \overline{V}_{H_2O} \nabla p_l \,, \tag{6}$$

where N is the water flux, κ_I is the ionic conductivity of PEM, ψ is the electro-osmotic coefficient, ξ is the water transport coefficient and $\overline{V}_{H_2O}$ is the molar volume of water.

The charge balances of electrons and ions can be represented by Poisson's equation [8, 9]:

$$-\nabla \cdot (\sigma \nabla \phi) + \mathcal{S} = 0 \,, \tag{7}$$

where σ is the electric/ionic conductivity, ϕ is the electric/ionic potential and $\mathcal{S}$ is the source term. The transport of electrons append in both the anode and cathode (domain $\Omega_{cPTL} \cup \Omega_{cCL}$ and $\Omega_{aCL} \cup \Omega_{aPTL}$), while the transport of ions occurs only in the membrane and the catalyst layers (domain $\Omega_{cCL} \cup \Omega_M \cup \Omega_{aCL}$), though inside the membrane (6) is used.

2.2. *Electrochemical description*

The source term in the charge balance equation (7) and the reaction term in the mass balance equation (1) are given by the Butler-Volmer kinetics, which describe the electrochemical reactions occurring at the catalyst layers. The Butler-Volmer equation describes the *interfacial current density* and is expressed as [9]:

$$i^r = s_l^r \cdot i_{0,ref}^r \exp\left[-\frac{E_r^0}{R}\left(\frac{1}{T} - \frac{1}{T_{\text{ref}}}\right)\right] \cdot \\ \cdot \left[\exp\left(\frac{z_r \alpha_r F \eta}{RT}\right) - \exp\left(\frac{z_r(\alpha_r - 1) F \eta}{RT}\right)\right] , \tag{8}$$

where $r \in \{\text{HER, OER}\}$ is the reaction qualifier, s_l^r is the saturation of the liquid phase, $i_{0,ref}^r$ is the reference exchange current density, E_r^0 is the standard electrode potential, R is the universal gas constant, T is the temperature, T_{ref} is the reference temperature, z_r is the charge number in the reaction, α_r is the transfer coefficient, η is the overpotential and F is Faraday's constant. The overpotential η is defined as the difference between the actual potential and the equilibrium potential of the reaction:

$$\eta = \phi_s - \phi_e - \phi_r^0 \,, \tag{9}$$

where ϕ_r^0 is the equilibrium potential of the reaction [9].

The reaction and source terms are also related to the *roughness factor* γ_M, which represents the surface area of the catalyst layer available for the reaction compared to the geometric area: it depends on the specific material used in the catalyst layer, usually platinum in the cathode and iridium in the anode [10].

Following [9], we define the reaction and source terms as follows:

$$\mathcal{R}_\alpha^\iota = \frac{\gamma_M}{l_r} \cdot \frac{M^\iota}{z_r F} \cdot i^r \,, \tag{10}$$

$$\mathcal{S} = \pm \frac{\gamma_M}{l_r} \cdot i^r \,, \tag{11}$$

where l_r is the thickness of the catalyst layer, M^ι is the molar mass of specie ι, i^r is the interfacial current density given by (8), and $\mathcal{S}$ is positive in the electronic equation and negative in the ionic equation.

2.3. *Assumptions*

We propose a 1D multiphysics multiscale model, inspired by Lin *et al.* [9]. The one-dimensional approach offers a balanced compromise between model complexity and physical insight: while simpler than a full 3D model, it still captures the essential dynamics in both time and space that lead to transition phases; indeed, this assumption is based on the prior that both the mass transfers and the charge/ion flows append mostly along the normal direction of the layers.

The one-dimensional domain is divided in 5 subdomains as showed in Figure 1, each of them represent a layer of the PEMWE. The model relies on several key assumptions. We consider the PEMWE cell to be isothermal with a fixed ambient temperature and pressure of 1 atm. Both the ionomers and the PEM are assumed to be fully wet in a quasi-liquid-equilibrated state. The liquid saturations at the flow channels are maintained constant, with boundary liquid saturations determined by the porous transport layers (PTL) pore structure and water flow rate in the channels. Additionally, we assume that the PEM does not allow gas to freely transport through the membrane, and that the water vapour partial pressure consistently equals the saturation pressure.

The last assumption is motivated by a time-scale separation: since the phase transition occurs on a much faster time scale compared to the one at which we can compute solutions for our system of equations, we model the phase change as instantaneous, with equilibrium conditions being continuously maintained.

3. NUMERICAL IMPLEMENTATION

The model and its numerical resolution are implemented in Python using the FEniCS[2] open-source computing platform. The finite element method is employed to discretize and solve the system of partial differential equations, allowing for flexible handling of complex multiphysics couplings and domain geometries. This approach ensures full reproducibility and extensibility of the modeling workflow, overcoming the limitations of commercial software and facilitating integration with advanced data-driven techniques.

The complete multiphysics system is solved using the iterative Algorithm 1 that exploits the time-scale separation between electrochemical and transport phenomena. At each time step, the electrochemical equations (6) and (7) are solved as steady-state problems, while the transport equations (1) and (4) are advanced in time in the anode and cathode domains. The coupling is achieved through boundary conditions at domain interfaces and reaction source terms updated at each iteration.

4. RESULTS AND DISCUSSION

4.1. *Electric and Ionic Potential Distributions*

We have successfully solved the electrochemical potential distributions in their respective domains using the numerical

[2] https://fenicsproject.org/

Algorithm 1 Iterative Multiphysics Coupling Algorithm

1: Initialize fluid dynamics variables and boundary conditions
2: **for** each time step **do**
3: Solve steady-state electrochemical system with current fluid state
4: Update reaction source terms from converged electrochemical fields
5: Advance transport equations by one time step
6: **end for**

framework described in Algorithm 1. Specifically, we have implemented the steady-state electrochemical system solver corresponding to line 3 of the algorithm.

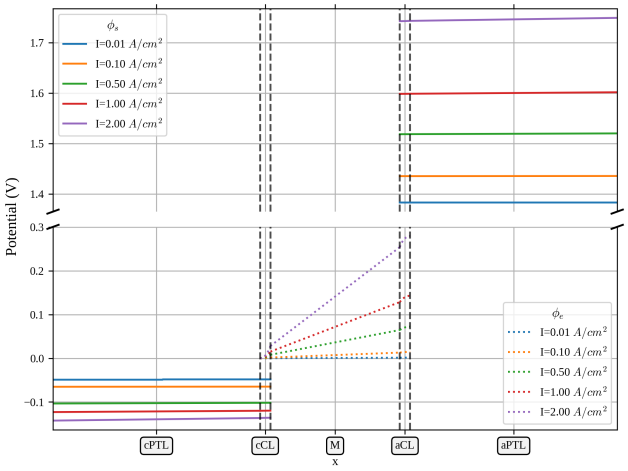

Figure 2. Spatial distribution of electric and ionic potentials across the 1D PEMWE domain for different values of I_{app}.

The electrochemical model described in the previous sections has been solved using spatially averaged and constant values for the fluid variables (saturation and pressures), which provides a foundation for understanding the potential distributions across the different domains of the PEMWE. The boundary conditions applied for the electrochemical problem are:

$$\mathbf{n} \cdot (-\sigma \nabla \phi_s) = I_{\text{app}} \quad \text{at } \Omega_{cPTL} \cap \text{ch} \tag{12}$$
$$\phi_e = 0 \quad \text{at } \Omega_{cPTL} \cap \Omega_{cCL} \tag{13}$$
$$-\sigma \nabla \phi_s = 0 \quad \text{at } \Omega_{cCL} \cap \Omega_M \tag{14}$$
$$-\sigma \nabla \phi_s = 0 \quad \text{at } \Omega_M \cap \Omega_{aCL} \tag{15}$$
$$-\kappa \nabla \phi_e = 0 \quad \text{at } \Omega_{aCL} \cap \Omega_{aPTL} \tag{16}$$
$$\mathbf{n} \cdot (-\sigma \nabla \phi_s) = I_{\text{app}} \quad \text{at } \Omega_{aPTL} \cap \text{ch} \tag{17}$$

The boundary conditions represent the electrical behavior at different interfaces of the PEMWE. Equations (12) and (17) apply the external current density at the cathode and anode flow channels, respectively, representing the electrical connection where current enters and exits the cell. Equation (13) sets the ionic potential to zero as a reference point, establishing the potential scale for the electrochemical system. Equations (14) and (15) ensure that electrons do not cross into or out of the membrane, as only ionic conduction occurs within the PEM. Finally, equation (16) prevents ionic current from entering the porous transport layer, where only electronic conduction should occur.

Figure 2 displays the simulated potential distributions for various applied current densities I_{app}. The detailed behavior of the solutions and the enforcement of boundary conditions are illustrated in Figure 3, which highlights the case with $I_{\text{app}} = 1\,\text{A/cm}^2$.

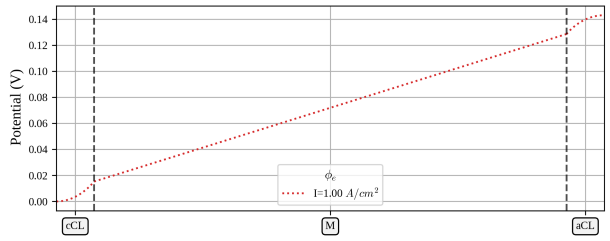

(a) Electrolyte-phase potential ϕ_e

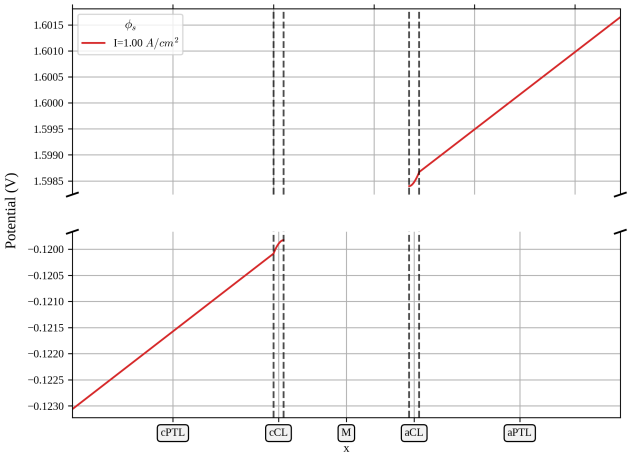

(b) Solid-phase potential ϕ_s

Figure 3. Spatial distributions of potentials across the 1D PEMWE domain for $I_{\text{app}} = 1\,\text{A/cm}^2$.

4.2. *Polarization Curves*

Figure 4 presents the polarization curve obtained from the 1D resolution, showing the relationship between applied current density and cell voltage.

To validate our approach and understand the advantages of spatial resolution, we compare our results with a simplified 0D model implemented following [11]. This comparison confirms the observations reported by [9]: the one-dimensional distribution of overpotentials contributes to higher overall cell potential values, even though the spatially-averaged overpotentials are equivalent to those predicted by the 0D model, as Figure 5 shows. This phenomenon occurs because of the nonlinear relationship between overpotential and current density in the Butler-Volmer kinetics. As a result, spatial variations in overpotential, even when the average remains the same, lead to different integrated electrochemical behavior.

The difference in the Ohmic losses, as can be seen from Figure 5, is consistent with the findings reported by [9] and is likely attributed to the linear representation of the phenomenon in the 0D model. As evident from the ionic potential distribution ϕ_e shown in Figure 3a, the spatial behavior is clearly non-linear across the membrane domain. The 0D model assumes a uniform linear potential drop, while the 1D spatial resolution reveals the actual non-linear potential gradients that occur due to varying ionic conductivity and local electrochemical conditions throughout the membrane thickness. This spatial heterogeneity in the ionic transport leads to higher effective resistance and consequently increased Ohmic losses compared to the simplified linear approximation used in 0D models.

This theoretical advantage of the 1D model is corroborated

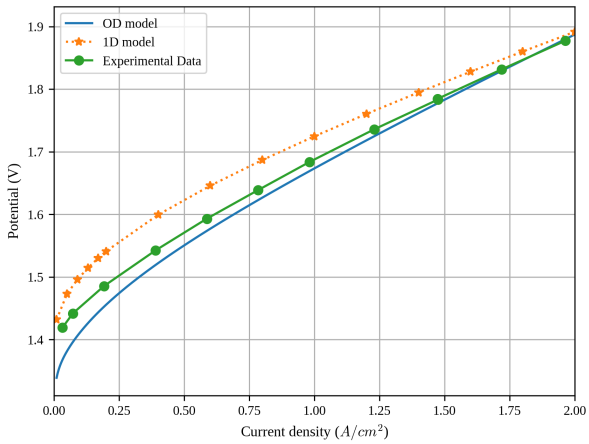

Figure 4. Polarization curves.

by preliminary comparison with experimental data. As shown in Figure 4, the experimental curve lies between the 0D and 1D model predictions, with the 1D model capturing better the sharp initial rise in cell voltage that characterizes real PEMWE behavior. At low current densities, the 1D model predicts a steeper voltage increase that more closely matches the experimental trend, suggesting that spatial heterogeneity effects are indeed significant in this operating regime. This improved agreement demonstrates the potential of the 1D approach to provide more accurate predictions, even without detailed parameter calibration, due to its better representation of the underlying physics through spatial resolution of overpotential distributions.

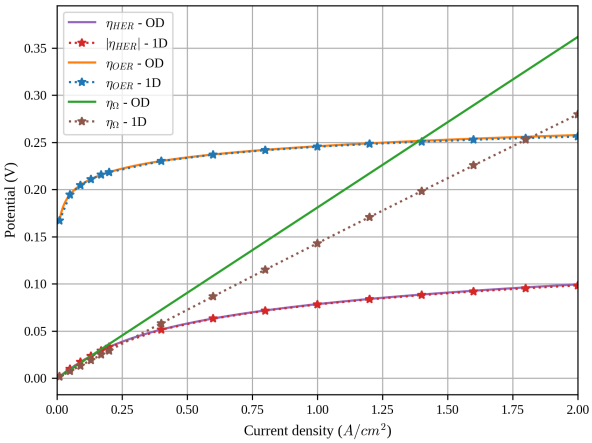

Figure 5. Comparison of overpotentials between the 0D and 1D models across different current densities.

5. CONCLUSIONS

In this work we present a 1D multiphysics model for a PEMWE, integrating mass transport in porous media with charge balance dynamics. The model considers both chemical and physical phenomena, focusing on phase transitions between liquid and gas states.We implement the resolution of the electric and ionic potentials in FEniCS and compare it against experimental I-V curves and existing 0D models.

The 1D model's ability to capture spatial effects provides valuable insights into the local electrochemical conditions within the catalyst layers, which can crucial for understanding degradation mechanisms and optimizing operating strategies. This spatial resolution becomes particularly important when considering the heterogeneous nature of phase transitions and local thermodynamic conditions that influence component durability.

The results presented here remains a partial implementation of the complete multiphysics system: the development of the mass transport equations is essential to achieve a fully functional model. The complete resolution of the coupled mass transport phenomena described in equations (1) and (4) will enable the study of phase transitions and their impact on PEMWE degradation mechanisms, which constitutes the ultimate objective of this research.

For the future work, we will validate the model by comparing its predicted I-V curves with experimental data. The I-V curve, representing the relationship between current density and voltage, is a fundamental characteristic of PEMWE performance and serves as an initial indicator of the model's global accuracy. However, while necessary, I-V curve validation alone does not guarantee that the model accurately captures all physical phenomena, particularly the phase transitions we aim to study. A more comprehensive validation would require additional experimental techniques, such as electrochemical impedance spectroscopy (EIS), to verify the internal detailed processes. The investigation of these aspects through EIS is beyond the scope of this work and is left for future research.

This first study lays the foundations to obtain a reliable real-time model, since the next step consists to implement a reduced model using neural network methodology, based on the proposed PDEs and numerical data produced by this validated numerical model. The *physical informed machine learning* approach [12] will be employed. This approach involves neural networks as basic technology and consists in the implementation of physical knowledge within neural models; this makes it possible to take advantage of the interpolatory capabilities, which these naturally possess, and to improve their predictive capabilities, since the results that the models produce must have a strong physical connotation.

Such accelerated model will be useful in PEMWE real-time control, helping for further study of the degradation process.

6. ACKNOWLEDGEMENTS

The authors gratefully acknowledge TARDY Erwan, BENHAMAD Maha, and DRUART Florence from the LEPMI laboratory in Grenoble for their valuable inputs and fruitful discussions that enhanced this work.

7. BIBLIOGRAPHY

[1] Q. Feng, X.-Z. Yuan, G. Liu, B. Wei, Z. Zhang, H. Li, and H. Wang, «A Review of Proton Exchange Membrane Water Electrolysis on Degradation Mechanisms and Mitigation Strategies», Journal of Power Sources, vol. 366, pp. 33-55, Oct. 2017.

[2] F. N. Khatib, T. Wilberforce, O. Ijaodola, E. Ogungbemi, Z. El-Hassan, A. Durrant, J. Thompson, and A. G. Olabi, «Material Degradation of Components in Polymer Electrolyte Membrane (PEM) Electrolytic Cell and Mitigation Mechanisms: A Review», Renewable and Sustainable Energy Reviews, vol. 111, pp. 1-14, Sep. 2019.

[3] M. Chandesris, V. Médeau, N. Guillet, S. Chelghoum, D. Thoby, and F. Fouda-Onana, «Membrane Degradation in PEM Water Electrolyzer: Numerical Modeling and Experimental Evidence of the Influence of Temperature and Current Density», International Journal of Hydrogen Energy, vol. 40, no. 3, pp. 1353-1366, Jan. 2015.

[4] S. M. Alia, S. Stariha, and R. L. Borup, «Electrolyzer Durability at Low Catalyst Loading and with Dynamic Operation», Journal of The Electrochemical Society, vol. 166, no. 15, pp. F1164-F1172, 2019.

[5] C. T. Miller, G. Christakos, P. T. Imhoff, J. F. McBride, J. A. Pedit, and J. A. Trangenstein, «Multiphase Flow and Transport Modeling in Heterogeneous Porous Media: Challenges and Approaches», Advances in Water Resources, vol. 21, no. 2, pp. 77-120, Mar. 1998.

[6] C. Y. Wang and P. Cheng, «A Multiphase Mixture Model for Multiphase, Multicomponent Transport in Capillary Porous Media—I. Model Develop-

ment», International Journal of Heat and Mass Transfer, vol. 39, no. 17, pp. 3607-3618, Nov. 1996.

[7] A. Z. Weber and J. Newman, «Transport in Polymer-Electrolyte Membranes: II. Mathematical Model», Journal of The Electrochemical Society, vol. 151, no. 2, p. A311, Jan. 2004.

[8] C. Ziegler, H. M. Yu, and J. O. Schumacher, «Two-Phase Dynamic Modeling of PEMFCs and Simulation of Cyclo-Voltammograms», Journal of The Electrochemical Society, vol. 152, no. 8, p. A1555, 2005.

[9] N. Lin, S. Feng, and J. Wang, «Multiphysics Modeling of Proton Exchange Membrane Water Electrolysis: From Steady to Dynamic Behavior», AIChE Journal, vol. 68, no. 8, p. e17742, Aug. 2022.

[10] D. Bessarabov, H. Wang, H. Li, and N. Zhao (Eds.), *PEM Electrolysis for Hydrogen Production: Principles and Applications*, CRC Press, Boca Raton, 2016. See especially Chapter 12: "Modeling of PEM Water Electrolyzer", pp. 243–267.

[11] V. Liso, G. Savoia, S. S. Araya, G. Cinti, and S. K. Kær, «Modelling and Experimental Analysis of a Polymer Electrolyte Membrane Water Electrolysis Cell at Different Operating Temperatures», Energies, vol. 11, no. 12, p. 3273, Nov. 2018.

[12] G. E. Karniadakis, I. G. Kevrekidis, L. Lu, P. Perdikaris, S. Wang, and L. Yang, «Physics-Informed Machine Learning», Nature Reviews Physics, vol. 3, no. 6, pp. 422-440, May 2021.